



Article

# Effects of 5 MeV Proton Irradiation on Nitrided SiO<sub>2</sub>/4H-SiC MOS Capacitors and the Related Mechanisms

Dongxun Li <sup>1</sup>, Yuming Zhang <sup>1</sup>, Xiaoyan Tang <sup>1,\*</sup>, Yanjing He <sup>1,\*</sup>, Hao Yuan <sup>1</sup>, Yifan Jia <sup>2</sup>, Qingwen Song <sup>1</sup>, Ming Zhang <sup>3</sup> and Yimen Zhang <sup>1</sup>

<sup>1</sup> School of Microelectronics, Xidian University, The State Key Discipline Laboratory of Wide Band Gap Semiconductor Technology, Xi'an 710071, China; lidxun@126.com (D.L.); zhangym@xidian.edu.cn (Y.Z.); haoyuan@xidian.edu.cn (H.Y.); qwsong@xidian.edu.cn (Q.S.); ymzhang@xidian.edu.cn (Y.Z.)

<sup>2</sup> School of Electronic Engineering, Xi'an University of Posts and Telecommunications, Xi'an 710121, China; jiaiyifan@xupt.edu.cn

<sup>3</sup> Beijing Institute of Spacecraft System Engineering, Beijing 100094, China; 13426209018@139.com

\* Correspondence: xytang@mail.xidian.edu.cn (X.T.); yanjing072126@163.com (Y.H.)

Received: 10 June 2020; Accepted: 6 July 2020; Published: 8 July 2020



**Abstract:** In this paper the effects of 5 MeV proton irradiation on nitrided SiO<sub>2</sub>/4H-SiC metal–oxide–semiconductor (MOS) capacitors are studied in detail and the related mechanisms are revealed. The density of interface states (Dit) is increased with the irradiation doses, and the annealing response suggests that the worse of Dit is mainly caused by displacement effect of proton irradiation. However, the X-rays photoelectron spectroscopy (XPS) measurement shows that the quantity proportion of breaking of Si≡N induced by displacement is only 8%, which means that the numbers of near interface electron traps (NIETs) and near interface hole traps (NIHTs) are not significantly changed by the displacement effect. The measurements of bidirectional high frequency (HF) C-V characteristics and positive bias stress stability show that the number of un-trapped NIETs and oxide electron traps decreased with increasing irradiation doses because they are filled by electrons resulted from the ionization effect of proton irradiation, benefiting to the field effective mobility ( $\mu_{FE}$ ) and threshold voltage stability of metal–oxide–semiconductor field-effect transistors (MOSFETs). The obviously negative shift of flat-band voltage ( $V_{FB}$ ) resulted from the dominant NIHTs induced by nitrogen passivation capture more holes produced by ionization effect, which has been revealed by the experimental samples with different nitrogen content under same irradiation dose.

**Keywords:** SiO<sub>2</sub>/4H-SiC MOS capacitors; proton irradiation; ionization effect; displacement effect; interface traps; near interface traps; flat-band voltage

## 1. Introduction

Because of the excellent electrical and thermal properties, silicon carbide (SiC) is a promising wide-bandgap semiconductor material with application in the power, high temperature, and space electronic fields [1,2]. With the improvement of the  $\mu_{FE}$  caused by the nitrogen passivation of SiC/SiO<sub>2</sub> interface, high voltage power metal–oxide–semiconductor field-effect transistor (MOSFET) switches have been available in the commercial market since 2011. SiC-based power devices are expected to be used in aerospace domain for substantially saving weight and enhancing performance. But the different types of irradiations in space environment will change the device electrical characteristics or even lead to the permanent failures of devices. The SiC devices are hopeful to exhibit high radiation hardness due to its high displacement threshold energy and the wide bandgap. Therefore, more research interests are turned to the irradiation effect of the nitrided MOS capacitors and power MOSFETs. The previous

studies focused on the total dose radiation response of  $\gamma$ -ray and X-ray, which are only considered as ionization effect [3–10]. The negative shift of  $V_{FB}$  and threshold voltage ( $V_{TH}$ ) is the major problem due to the positive charges generated in the gate oxide during irradiation, but the mechanisms of formation of positive charges are required to be further studied. In addition, the effect of ionization irradiation on near interface traps which can significantly influence the  $\mu_{FE}$  of MOSFET has not been investigated.

Also, the displacement effect of irradiation on the devices is rarely reported, which can create defects to affect the electrical properties of the devices. Proton irradiation is one of the main particles in space environment, and will make both the ionization effect and displacement effect. So it is required to study the effects of proton irradiation on nitrided MOS capacitor and MOSFET for space applications. The previous report of proton irradiation based on the lateral MOSFETs only concentrated on the proton irradiation effects on the  $\mu_{FE}$  and  $V_{TH}$ , in which  $\mu_{FE}$  is improved and  $V_{TH}$  is decreased with increasing doses, but the relative mechanisms are still unclear [11].

Therefore, in this paper the effects of 5 MeV proton irradiation on nitrided  $\text{SiO}_2/4\text{H-SiC}$  MOS capacitors are studied in detail and the related mechanisms are revealed. With the analysis of the XPS measurement and annealing response of the samples, the ionization effect and displacement effect of proton irradiation on interface traps and near interface traps are clarified, and the mechanisms of the variation of the  $\mu_{FE}$  are understood. By the experiments of the samples with different nitrogen content under same irradiation dose, the nitrogen passivation induced the shift of  $V_{FB}$  under irradiation is revealed. Finally, the gate oxide integrity, free carrier concentration ( $n_D$ ) in epilayer and positive bias stress stability of  $V_{FB}$  are also discussed, which are important for the power MOSFET.

## 2. Experiments

### 2.1. Test Devices

The MOS capacitors under test were fabricated on a 4H-SiC epilayer with thickness of 5  $\mu\text{m}$  and nitrogen-doped concentration of  $1.77 \times 10^{16} \text{ cm}^{-3}$ , grown on a  $4^\circ$  off-axis  $\text{N}^+$  type 4H-SiC substrate with thickness of 350  $\mu\text{m}$ . Following the RCA cleaning, an HF dip, water rinsing, and thermal oxidation were carried out in a dry  $\text{O}_2$  environment at a temperature of 1300  $^\circ\text{C}$ . Afterwards, post oxidation NO annealing was performed under the condition of 1175  $^\circ\text{C}$  for 2 h. The thickness of the gate oxide is about 35 nm measured by spectroscopy ellipsometry (SE). Finally, nickel was evaporated for the backside ohmic contact and aluminum was sputtered on the oxide surface to form the gate electrode. The diameter of the gate electrode is 50  $\mu\text{m}$ . In order to analyze the mechanisms of the shift of  $V_{FB}$  under proton irradiation, the samples were fabricated with changing annealing temperature and time, which are respectively 1100  $^\circ\text{C}$  with 1 h and 2 h, and 1250  $^\circ\text{C}$  with 1 h and 2 h. Schematic diagram of the nitrided  $\text{SiO}_2/4\text{H-SiC}$  MOS capacitor is shown in Figure 1. The current to voltage (I-V) characteristics and HF (100 kHz) capacitance-voltage (C-V) measurements were measured on a CASCADE probe station using a Keysight B1505A semiconductor parameter analyzer at room temperature prior to the irradiation.

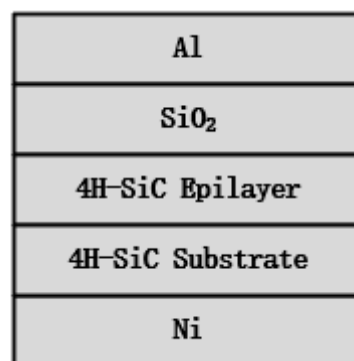


**Figure 1.** Schematic diagram of the nitrided  $\text{SiO}_2/4\text{H-SiC}$  metal–oxide–semiconductor (MOS) capacitors.

## 2.2. High Energy Proton Irradiation

Unbiased devices were irradiated with 5 MeV protons using the EN2 × 6 serial electrostatic accelerator (High Voltage Engineering Europa B.V., Amersfoort, Netherlands). The vertical irradiation to surface of the samples was performed in vacuum atmosphere at room temperature with the proton fluences of  $5 \times 10^{12}$  p/cm<sup>2</sup>,  $2 \times 10^{13}$  p/cm<sup>2</sup>,  $5 \times 10^{13}$  p/cm<sup>2</sup>,  $1 \times 10^{14}$  p/cm<sup>2</sup>, and  $5 \times 10^{14}$  p/cm<sup>2</sup> under the same proton fluence rate of  $1.39 \times 10^{10}$  p/(cm<sup>2</sup>·s), respectively. The proton energy was chosen from the energy range of protons in space environment, which is similar to the previous research on the irradiation effects of protons on 4H-SiC epilayers and MOSFETs [11,12]. The maximum incident depth is approximately 149 μm located in the substrate, which is determined by the Monte Carlo simulations using the SRIM software, as shown in Figure 2 [13]. According to the SRIM simulation of the ionization energy loss and the number of target vacancies versus the depth, the ionization effect and displacement effect of proton irradiation occur along the path of the injected protons during the proton irradiation. In order to analyze the mechanisms of the shift of  $V_{FB}$  under proton irradiation, the samples with different nitrogen contents were irradiated with the same dose of  $2 \times 10^{13}$  p/cm<sup>2</sup>. The I-V characteristics and C-V characteristics of these devices were re-measured at room temperature 24 h after each proton irradiation. The measurements of positive bias stress stability of  $V_{FB}$  were applied by positive bias stress of 3 MV/cm for the stress time in the range of 0–600 s, followed by HF (100 kHz) C-V measurements.

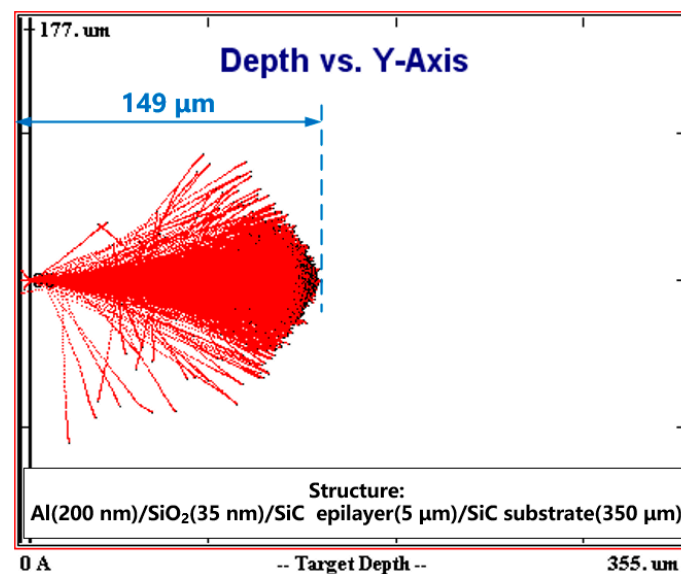


Figure 2. SRIM simulation of the MOS Capacitors injected by a 5MeV Proton beam.

## 2.3. XPS Measurement and Annealing Experiment

XPS measurements were performed using a Thermo Scientific XPS (ESCALAB 250Xi) system, equipped with an Al K $\alpha$  radiation source (1486.6 eV) for the excitation of photoelectrons. Argon ion sputtering was carried out in the same ultrahigh-vacuum chamber to remove the SiO<sub>2</sub> layer gradually. The isochronal annealing experiments were performed in air ambient without gate bias at temperatures from 50 °C to 150 °C with each step of 50 °C [14]. The samples were held in 1 h, and then sequentially processed for total 3 h at the respective temperatures before cooling back down to room temperature for C-V characteristics measurements.

### 3. Results and Discussion

#### 3.1. Gate Oxide Integrity

The HF C-V characteristics of the samples irradiated by proton doses are shown in Figure 3, in which the gate voltage was swept from depletion to accumulation. It can be seen that the samples were failed in the C-V characteristics when the irradiation dose is up to  $1 \times 10^{14}$  p/cm<sup>2</sup>. To evaluate the irradiation effect on the gate oxide integrity, the forward I-V characteristics were measured at room temperature by sweeping the gate voltage up to 35 V. The forward current versus electric field (I-E) of the samples with different doses of proton irradiation is shown in Figure 4, which is transformed from the measured I-V characteristics. It can be observed that the leakage current of the samples irradiated by the dose up to  $5 \times 10^{13}$  p/cm<sup>2</sup> remains very little value as the electric field is smaller than 6 MV/cm, resulted from the direct tunneling of the oxide layer, and rapidly increases because of Fowler-Nordheim (F-N) tunneling, complied with F-N rule as the electric field higher than 6 MV/cm. But the leakage current of the samples irradiated by the dose over  $5 \times 10^{13}$  p/cm<sup>2</sup> is increased obviously with the increasing irradiated doses in the low electric field and not complied with F-N rule in the high electric field, which could be owing to the damage of the barrier between SiO<sub>2</sub> and 4H-SiC caused by the defects in the oxide layer generated by the displacement effect of proton irradiation, and this is also the reason lost C-V characteristic for the samples after irradiation dose of  $1 \times 10^{14}$  p/cm<sup>2</sup>. Therefore, this could lead to the failure of the MOSFET due to losing gate control.

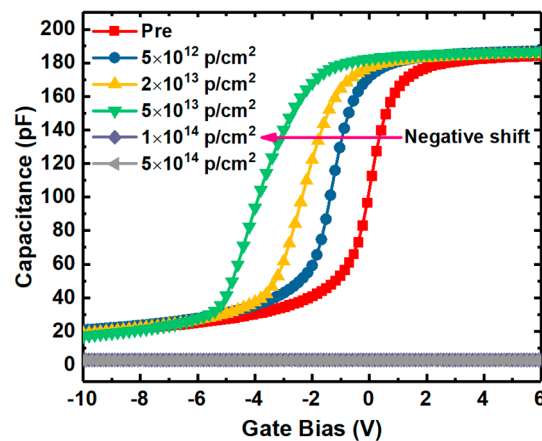


Figure 3. High frequency (HF) C-V characteristics of the samples irradiated by proton doses.

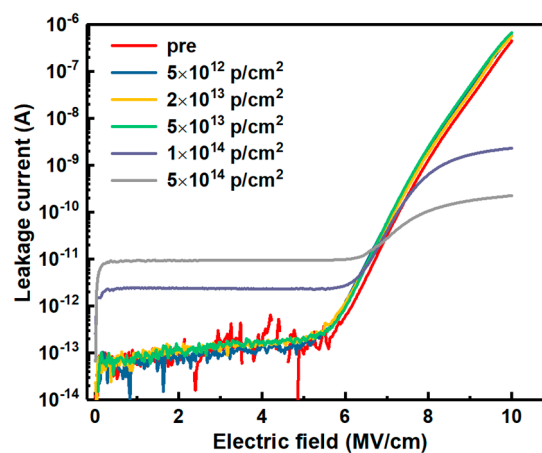


Figure 4. Typical current versus electric field of the samples with different doses of proton irradiation.

### 3.2. Free Carrier Concentration

The  $n_D$  in the epilayer versus proton fluence is extracted by HF C-V characteristics of the samples, as shown in Figure 5. It can be seen that the  $n_D$  is reduced with increasing irradiation dose. The previous experiment showed that the displacement effect of the proton irradiation introduces several electron traps and their energy levels are located at 0.18 eV, 0.2 eV, 0.4 eV, 0.72 eV, 0.76 eV, and 1.09 eV below the conduction-band edge, respectively [12], which measured on the 6.5 MeV proton-irradiated 4H-SiC epilayer using deep-level transient spectroscopy (DLTS), which is almost of similar energy and range of doses as our experiment. The concentrations of the defects are linearly related to irradiation dose. These electron traps capture free carrier, resulting in the  $n_D$  reduced as carrier removal effect. This effect could significantly influence the ON-state resistance of the power MOSFET, finally leading to the failure of the device by worsening of the resistivity of lightly doped drift region and the pinching off of JFET region.

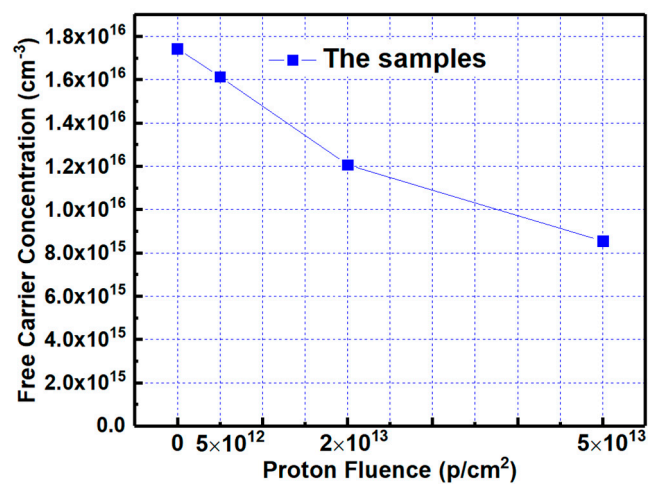
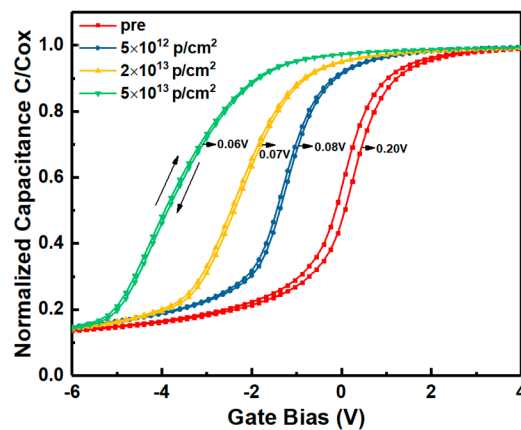


Figure 5. The free carrier concentration of the epilayer versus proton fluence.

### 3.3. Near Interface Traps

The normalized bidirectional HF C-V characteristics of the samples irradiated by proton doses are shown in Figure 6. In the measurements, the gate voltage was swept from depletion to accumulation, and then swept back to depletion. The hysteresis voltage ( $\Delta V$ ) is related to the un-trapped NIETs which could trap electrons at the accumulation condition [15]. The areal density of un-trapped NIETs can be calculated by  $(C_{ox}/qS) \cdot \Delta V$ , where  $C_{ox}$  is oxide capacitance,  $q$  is electronic charge,  $S$  is area of oxide capacitance, as shown in Table 1. It can be observed that the number of un-trapped NIETs is decreased with the increasing irradiation dose. However, the number of un-trapped NIETs is affected by the number and the trapping state (trapped or un-trapped state) of the NIETs. The former can be influenced by the displacement effect of proton irradiation and the latter can be affected by the ionization effect of proton irradiation.



**Figure 6.** Bidirectional HF C-V characteristics of the samples irradiated by proton doses.

**Table 1.** Extracted hysteresis voltage and the areal density of un-trapped NIETs of the samples irradiated by proton doses.

| Irradiation Dose (p/cm <sup>2</sup> ) | Hysteresis Voltage (V) | Areal Density of un-Trapped NIETs (cm <sup>-2</sup> ) |
|---------------------------------------|------------------------|---|
| pre                                   | 0.20                   | $1.2 \times 10^{11}$                                  |
| $5 \times 10^{12}$                    | 0.08                   | $4.7 \times 10^{10}$                                  |
| $2 \times 10^{13}$                    | 0.07                   | $4.2 \times 10^{10}$                                  |
| $5 \times 10^{13}$                    | 0.06                   | $3.6 \times 10^{10}$                                  |

To analyze the displacement effect on NIETs, the XPS measurements of the samples without irradiation and with the irradiation dose of  $5 \times 10^{13}$  p/cm<sup>2</sup> (the maximum irradiation dose before failure of the samples) were performed, in which argon ion sputtering was carried out to remove the SiO<sub>2</sub> layer gradually and each step of sputtering time is 10 s (about 0.8 nm in depths). The XPS spectra of Si 2p core level taken from the different depths of the transition layers from SiO<sub>2</sub> to SiC are shown in Figures 7 and 8, respectively. From this process the XPS spectra at the near interface can be obtained and compared. The results of deconvolution of the Si 2p core level XPS spectra at the near interface for the samples are shown in Figures 9 and 10, respectively. Before the curve fitting, Shirley background subtraction was performed and all spectra were charge compensated relative to the binding energy of the C-C bond (284.6 eV). Then XPS spectra were resolved as sums of several components taking each peak of a Gaussian distribution. Four main components are observed in the Si 2p spectra, which are Si-C, Si≡N, Si-O<sub>x</sub>, and SiO<sub>2</sub> located at 100.6 eV, 101.6 eV, 102.5 eV, and 103.4 eV binding energies, respectively. The relative contents of the intermediate oxidation state of Si-O<sub>x</sub> and Si≡N in the Si 2p core level spectra for the samples without irradiation and with irradiation dose of  $5 \times 10^{13}$  p/cm<sup>2</sup> are shown in Figure 11, obtained by XPS analysis software (Thermo Avantage). It can be seen that the content of Si-O<sub>x</sub> is increased slightly and Si≡N is decreased a little after irradiation. It can be considered that the breaking of Si≡N made by displacement effect of proton irradiation leads to more Si-O<sub>x</sub>, but the quantity is only 8%. Considering the NIET originates in Si-O<sub>x</sub> and the NIHT originates in Si≡N [16–18], the number of both traps is not significantly changed by the displacement effect. The trapping state of the NIETs can be markedly changed by trapping electrons during irradiation generated by the ionization effect along the path of the injected proton. Therefore, the decrease of the number of un-trapped NIETs after irradiation is mainly affected by the ionization effect of the proton irradiation, which can be beneficial to the  $\mu_{FE}$  of MOSFET [19–21].

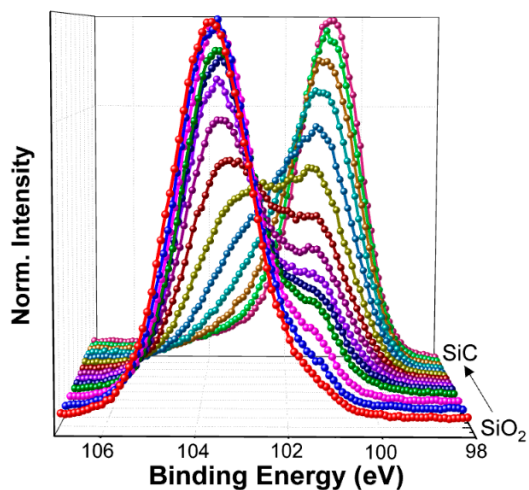


Figure 7. Si 2p core level X-rays photoelectron spectroscopy (XPS) spectra taken from the different depths of the transition of the sample without irradiation.

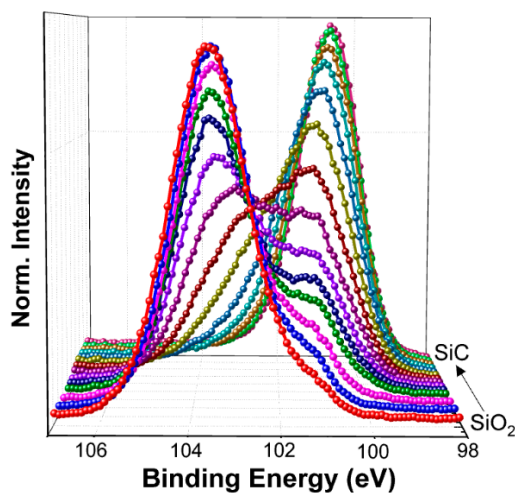


Figure 8. Si 2p core level XPS spectra taken from the different depths of the transition of the sample with the irradiation dose of  $5 \times 10^{13}$  p/cm<sup>2</sup>.

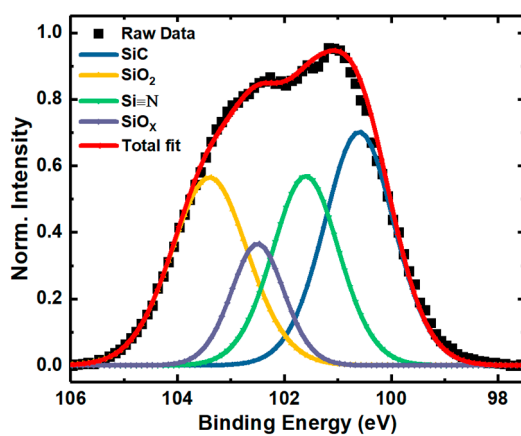
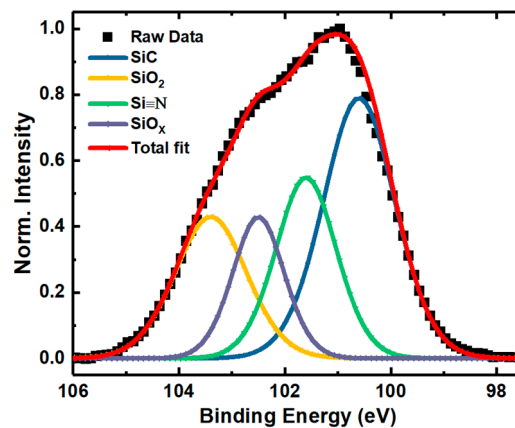
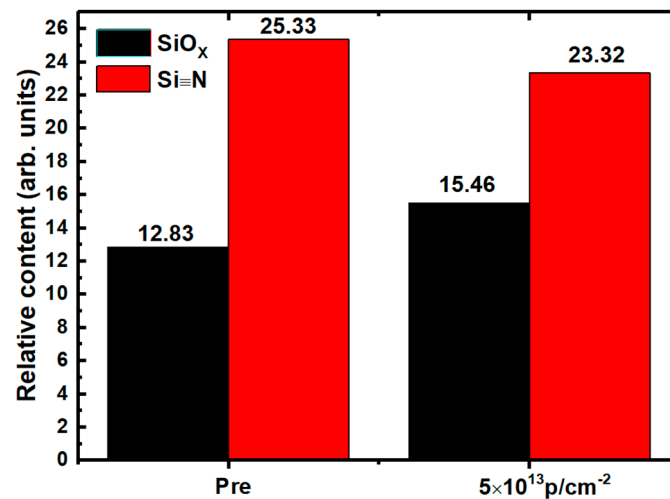


Figure 9. Si 2p core level XPS spectrum at the near interface of the samples without irradiation.



**Figure 10.** Si 2p core level XPS spectrum at the near interface of the samples with the irradiation dose of  $5 \times 10^{13}$  p/cm<sup>2</sup>.



**Figure 11.** The relative contents of silicon suboxide and silicon nitride in the Si 2p core level spectra of the samples without irradiation and with the irradiation dose of  $5 \times 10^{13}$  p/cm<sup>2</sup>.

### 3.4. Flat-Band Voltage

The shift of  $V_{FB}$  of the samples compared with the un-irradiation one versus proton fluence extracted from the HF C-V characteristics of the irradiated samples (in Figure 3) is shown in Figure 12. Before failure, the  $V_{FB}$  of the samples decreases obviously with the increase of irradiation dose and the shift of  $V_{FB}$  is  $-3.49$  V after the irradiation dose of  $5 \times 10^{13}$  p/cm<sup>2</sup>, which means a significant increment of the net positive charges nearby the SiO<sub>2</sub>/4H-SiC interface during irradiation. The schematic diagram of main traps affecting  $V_{FB}$  during irradiation nearby the SiO<sub>2</sub>/4H-SiC interface is shown in Figure 13. As discussed from XPS spectra above, the number of NIETs and NIHTs are not significantly changed by the displacement effect during proton irradiation. Therefore, the effect of proton irradiation on  $V_{FB}$  is mainly affected by the ionization effect of the proton irradiation, depending on the dominate traps near the interface which could be the oxide hole traps formed by the oxygen vacancy or NIHT induced by nitrogen passivation. So the samples with different nitrogen content varied by adjusting the NO annealing time were performed under same irradiation dose of  $2 \times 10^{13}$  p/cm<sup>2</sup>. The annealing time is respectively 1 h and 2 h at temperatures of 1100 °C and 1250 °C. HF C-V characteristics of the samples with different nitrogen content irradiated by same proton dose is shown in Figure 14. Considering the different thickness of oxide ( $t_{ox}$ ) of the samples, the extracted variation of the areal density of effective dielectric charge ( $\Delta N_{ef}$ ) of the samples is shown in Table 2. It can be seen that the  $\Delta N_{ef}$  of the samples with annealing time of 2 h are obviously more than that with 1 h under both

temperatures of 1100 °C and 1250 °C. It means that the  $\Delta N_{ef}$  is significantly related to the nitrogen content. The nitrogen passivation not only reduces the numbers of the NIETs but also generates a large number of the NIHTs, leading to the dominant hole traps nearby the SiO<sub>2</sub>/4H-SiC interface. When the protons penetrate through the devices the ionization effect of proton irradiation creates electron-hole pairs along the path of the injected proton. The dominant NIHTs capture more holes in this event, resulting in the generation of net positive charges nearby the SiO<sub>2</sub>/4H-SiC interface. This is the reason for the larger negative shift of  $V_{FB}$  after proton irradiation. This serious problem must be addressed because it could induce the MOSFETs to not turn off normally. Therefore, it is necessary for the nitrogen content controlling to carefully choose annealing condition to balance the improvement of  $\mu_{FE}$  induced by the decrease of NIETs and the shift of  $V_{TH}$  caused by the formation of NIHTs for the application of MOSFETs in ionization irradiation environment.

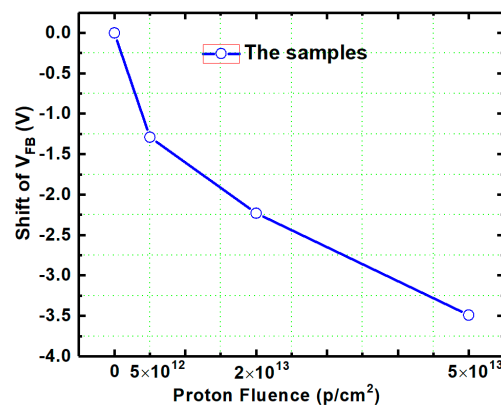


Figure 12. The shift of  $V_{FB}$  of the samples versus proton fluence extracted from the HFC-V characteristics.

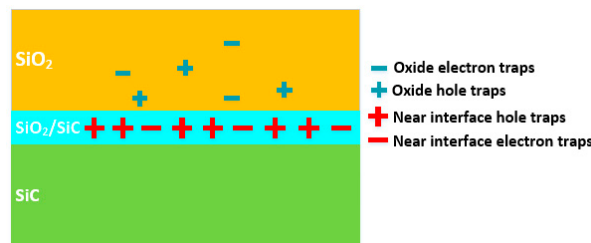
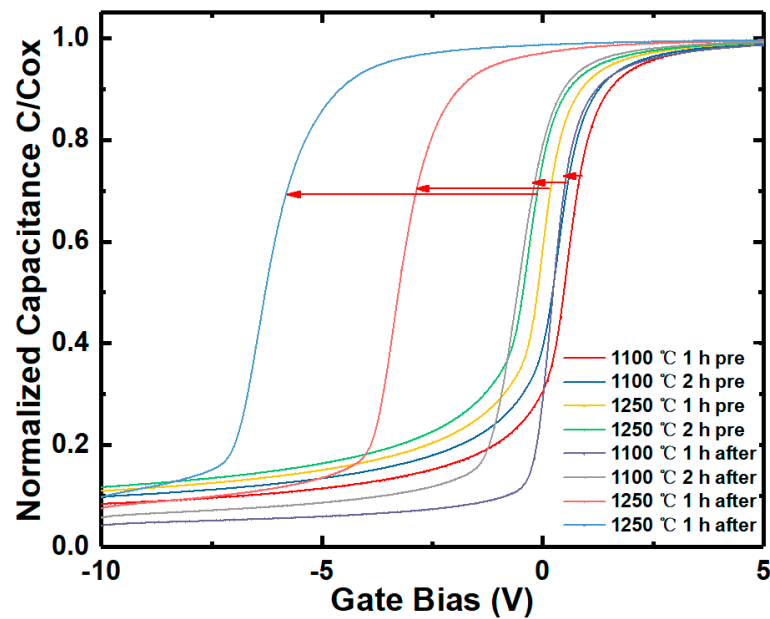


Figure 13. The schematic diagram of main traps affecting  $V_{FB}$  during irradiation nearby the SiO<sub>2</sub>/4H-SiC interface.

Table 2. Extracted the shift of  $V_{FB}$  and the variation of areal density of effective dielectric charge of the samples with different nitriding process irradiated by the same proton dose of  $2 \times 10^{13}$  p/cm<sup>-2</sup>.

| Annealing Condition | the Shift of $V_{FB}$ (V) | Tox (nm) | $\Delta N_{ef}$ (cm <sup>-2</sup> ) |
|---------------------|---------------------------|----------|-------------------------------------|
| 1100 °C 1 h         | 0.3                       | 48.0     | $1.4 \times 10^{11}$                |
| 1100 °C 2 h         | 0.9                       | 48.8     | $4.0 \times 10^{11}$                |
| 1250 °C 1 h         | 3.2                       | 52.8     | $1.3 \times 10^{12}$                |
| 1250 °C 2 h         | 5.9                       | 56.8     | $2.2 \times 10^{12}$                |



**Figure 14.** HF C-V characteristics of the samples with different nitriding process irradiated by same proton dose of  $2 \times 10^{13} \text{ p/cm}^{-2}$ .

### 3.5. Interface Traps

Energy distributions of interface states densities of the samples irradiated by proton doses obtained by Terman's method based on measured HF C-V characteristics (in Figure 3) are shown in Figure 15. It can be observed that the  $D_{it}$  is increased with the increasing irradiation dose. The displacement effect of the proton irradiation causes various types broken bonds between atoms, when the protons penetrate through the interface. The defects generated at the interface caused by the displacement effect could be the reason for the increase of  $D_{it}$ . But the worse of  $D_{it}$  is present in the irradiation of only ionization effect [3]. Which effect has more significant influence on  $D_{it}$  is analyzed by the annealing response of the samples without irradiation and with the irradiation dose of  $5 \times 10^{13} \text{ p/cm}^2$ . The HF C-V characteristics of the sample at different stages of the isochronal annealing are shown in Figure 16. The relationship between the  $n_D$  and annealing condition is shown in Figure 17. It can be seen that the  $n_D$  only returned to 29% of pre-irradiation levels after the isochronal annealing. The extracted  $V_{FB}$  of the sample at different stages of the isochronal annealing are showed in Figure 18. It can be noticed that the  $V_{FB}$  of the samples returned to 70% of pre-irradiation levels after the isochronal annealing. Energy distributions of  $D_{it}$  of the sample at different stages of the isochronal annealing are plotted in Figure 19. It can be seen that the recovery of  $D_{it}$  of the sample is 32% which is similar to the recovery of  $n_D$  (29%) mainly affected by the displacement effect and different from the recovery of  $V_{FB}$  (70%) mainly influenced by ionization effect, so it can be considered that the worse of  $D_{it}$  is mainly affected by the displacement effect of proton irradiation.

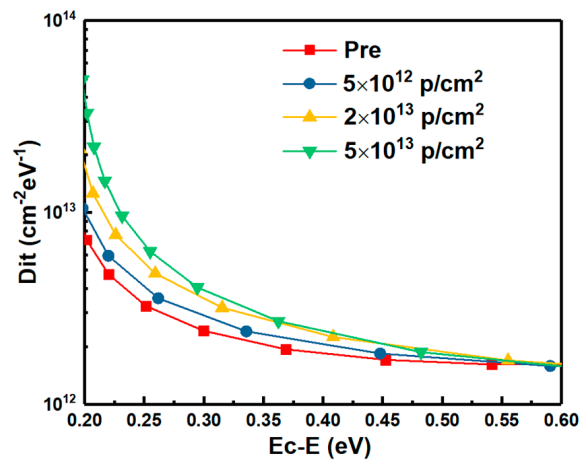


**Figure 15.** Energy distributions of interface states densities of the samples irradiated by proton doses obtained by Terman’s method.

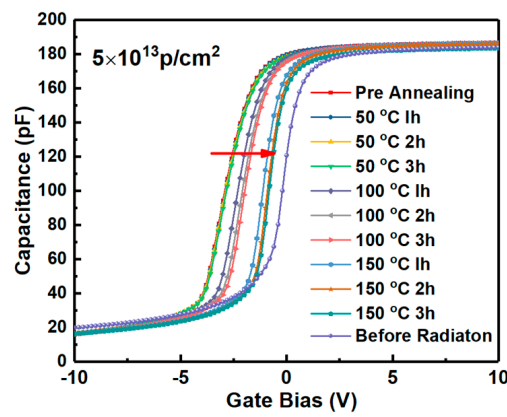


**Figure 16.** HF C-V characteristics of the samples at different stages of the isochronal annealing.

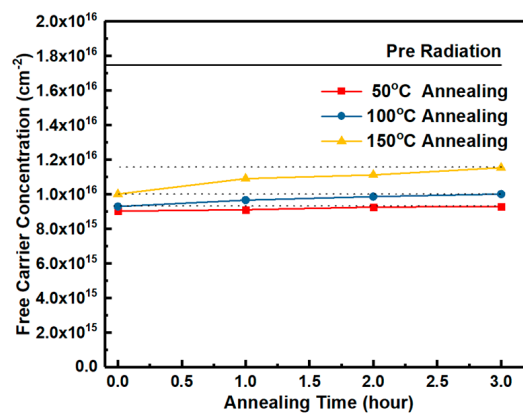


**Figure 17.** The extracted free carrier concentration of the epilayer at different stages of the isochronal annealing.

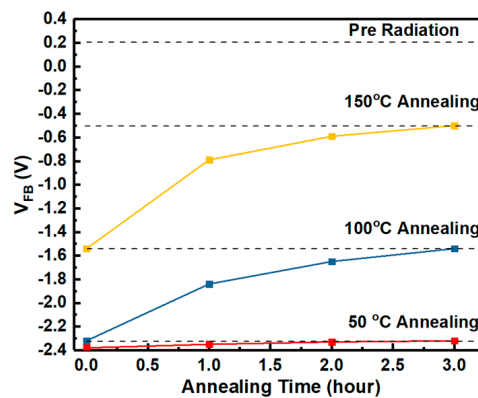


**Figure 18.** The extracted flat-band voltage of the sample at different stages of the isochronal annealing.

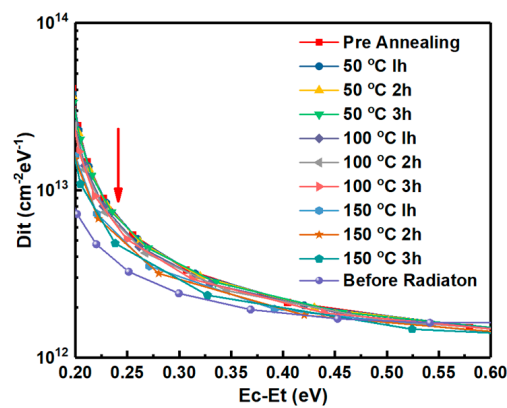


**Figure 19.** Energy distributions of interface states density in the sample at different stages of the isochronal annealing.

Up to now, the irradiation effect on NIETs and interface traps have been analyzed and it can be summarized in Figure 20. The  $\mu_{FE}$  of MOSFET is affected by the interface traps located close to the conduction band and the NIETs near the conduction band, and the effect of the latter one is more significant [19–21]. The electrons in the inversion layer can directly tunnel or tunnel via interface traps to the un-trapped NIETs when the MOSFET devices are biased into strong inversion, which reduce the number of channel conducting electrons resulting in the effective reduction of  $\mu_{FE}$ . This could explain the results of previous study, in which the  $\mu_{FE}$  of MOSFET irradiated by 5 MeV proton is increased with the increasing irradiation dose [11]. In this case, the reduction of the un-trapped NIETs by the ionization effect of proton irradiation could be the reason for the improvement of  $\mu_{FE}$  with increasing irradiation doses.

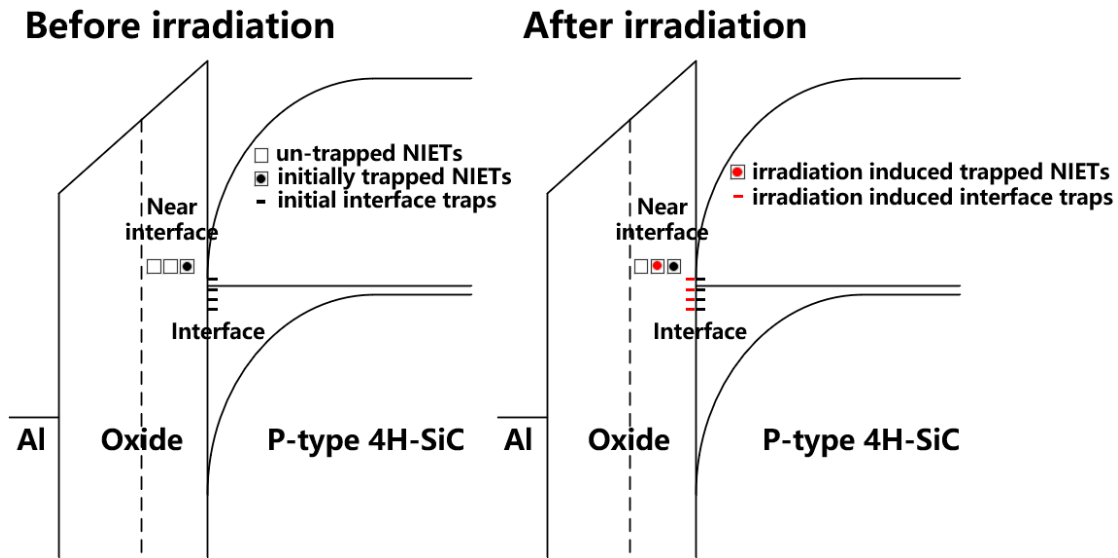


Figure 20. Energy band diagrams for the effect of proton irradiation on NIETs and interface traps.

### 3.6. The Positive Bias Stress Stability of $V_{FB}$

Electrons tunneling into the NIETs far away from the interface and oxide electron traps are hardly released quickly when suffering time-dependent bias stress (TDBS), resulting in the problem of the threshold voltage stability [22]. It has been confirmed that n-channel MOSFET operated in strong inversion (in a positive gate bias) can be equivalent to an n-type MOS capacitor in the accumulation state. Thus, it is necessary to investigate the irradiation effect on the positive bias stress stability of  $V_{FB}$ . The samples without irradiation and with the irradiation dose of  $5 \times 10^{13}$  p/cm<sup>2</sup> were applied by positive bias stress of 3 MV/cm for different stress time in the range of 0–600 s, followed by HF C-V measurements, as shown in Figures 21 and 22, respectively. The variation of  $V_{FB}$  ( $\Delta V_{FB}$ ) compared with the samples before the positive bias stress extracted from the C-V measurements of the samples versus the stress time is shown in Figure 23. Compared with the un-irradiated samples, the  $\Delta V_{FB}$  of the samples after irradiation is decreased after every stress time, which could be attributed to the NIETs far away from the interface and oxide electron traps filled by the electrons resulted from the ionization effect of proton irradiation. The decrease of  $\Delta V_{FB}$  after irradiation could contribute to the threshold voltage stability of n-channel MOSFETs.

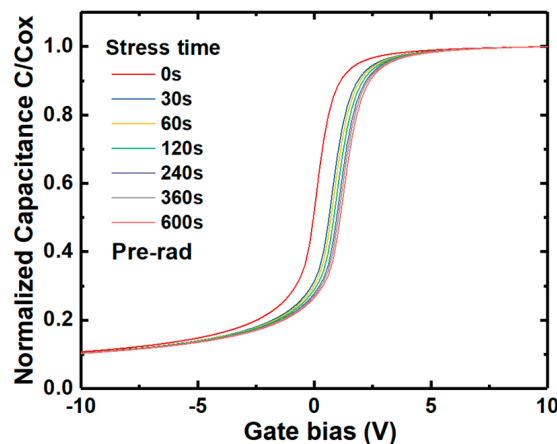
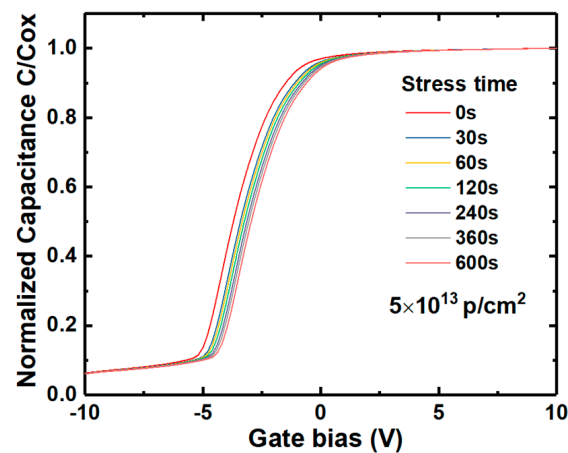
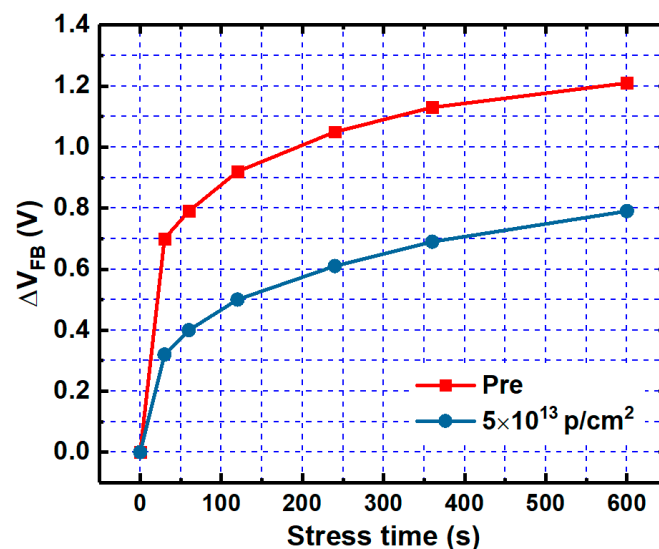


Figure 21. HF C-V characteristics of the un-irradiated samples with the stress time.



**Figure 22.** HF C-V characteristics of the samples irradiated by the dose of  $5 \times 10^{13}$  p/cm<sup>2</sup> with the stress time.



**Figure 23.** The variation of  $V_{FB}$  of the samples without irradiation and with the irradiation dose of  $5 \times 10^{13}$  p/cm<sup>2</sup> versus the stress time.

Up to now, the ionization effect on the electrical characteristics can be summarized as that traps present at the regions from SiO<sub>2</sub> to interface (shown in Figure 13) can be filled during irradiation caused by ionization effect, which could be beneficial to the  $\mu_{FE}$  and threshold voltage stability of n-channel MOSFETs, but cause serious problem of obvious negative shift of  $V_{FB}$  and  $V_{TH}$ .

#### 4. Conclusions

In this paper the effects of 5 MeV proton irradiation on nitrated SiO<sub>2</sub>/4H-SiC MOS capacitors are studied in detail and the related mechanisms are revealed. Because of the displacement effect of proton irradiation in the oxide, the gate oxide integrity is broken after the irradiation dose of  $5 \times 10^{13}$  p/cm<sup>2</sup>, which could lead to the failure of power MOSFET. The  $D_{it}$  is increased with the irradiation doses, and the annealing response suggests that the worse of  $D_{it}$  is mainly caused by displacement effect of proton irradiation. However, the XPS measurement shows that the quantity proportion of breaking of Si≡N induced by displacement is only 8%, which means that the numbers of NIETs and NIHTs are not significantly changed by displacement effect. The measurements of bidirectional HF C-V characteristics and positive bias stress stability show that the number of un-trapped NIETs and oxide electron traps decreased with increasing irradiation doses because they are filled by electrons resulted

from the ionization effect of proton irradiation, benefiting to the  $\mu_{FE}$  and threshold voltage stability of MOSFETs. The obviously negative shift of  $V_{FB}$  resulted from the dominant NIHTs induced by nitrogen passivation capture more holes produced by ionization effect, which has been revealed by the experimental samples with different nitrogen content under same irradiation dose. This serious problem must be addressed because it could induce the MOSFETs to be not turned off normally. Therefore, it is necessary for nitrogen content controlling to carefully choose annealing condition to balance the improvement of  $\mu_{FE}$  induced by the decrease of both of NIETs and the shift of  $V_{TH}$  caused by the formation of NIHTs for the application of MOSFETs in ionization irradiation environment.

**Author Contributions:** Conceptualization, D.L.; methodology, D.L.; software, D.L.; validation, D.L., X.T., Y.Z. (Yuming Zhang), and Y.H.; formal analysis, D.L.; investigation, D.L.; resources, Y.H., H.Y., Y.J., and M.Z.; data curation, D.L.; writing—original draft preparation, D.L.; writing—review and editing, X.T. and Y.Z. (Yimen Zhang); visualization, D.L.; supervision, Y.Z. (Yuming Zhang) and X.T.; project administration, Y.Z. (Yuming Zhang) and X.T.; funding acquisition, X.T., Y.Z. (Yuming Zhang), H.Y., Q.S. All authors have read and agreed to the published version of the manuscript.

**Funding:** This research was funded by Science Challenge Project (Grant No. TZ2018003), National Natural Science Foundation of China (Grant No. 61774119, No. 61774117 and No. 61804118) and Key-Area Research and Development Program of Guang Dong Province (Grant No. 2020B010170001).

**Conflicts of Interest:** The authors declare no conflict of interest.

## References

- Cooper, J.A.; Agarwal, A. SiC power-switching devices—the second electronics revolution? *Proc. IEEE* **2002**, *90*, 956–968. [\[CrossRef\]](#)
- Cooper, J.A.; Melloch, M.R.; Singh, R.; Agarwal, A.; Palmour, J.W. Status and prospects for SiC power MOSFETs. *IEEE Trans. Electron Devices* **2002**, *49*, 658–664. [\[CrossRef\]](#)
- Dixit, S.K.; Dhar, S.; Rozen, J.; Wang, S.; Schrimpf, R.D.; Fleetwood, D.M.; Pantelides, S.T.; Williams, J.R.; Feldman, L.C. Total dose radiation response of nitrided and non-nitrided SiO<sub>2</sub>/4H-SiC MOS capacitors. *IEEE Trans. Nucl. Sci.* **2006**, *53*, 3687–3692. [\[CrossRef\]](#)
- Arora, R.; Rozen, J.; Fleetwood, D.M.; Galloway, K.F.; Zhang, C.X.; Han, J.; Dimitrijević, S.; Kong, F.; Feldman, L.C.; Pantelides, S.T.; et al. Charge trapping properties of 3C- and 4H-SiC MOS capacitors with nitrided gate oxides. *IEEE Trans. Nucl. Sci.* **2009**, *56*, 3185–3191. [\[CrossRef\]](#)
- Zhang, C.X.; Zhang, E.X.; Fleetwood, D.M.; Schrimpf, R.D.; Dhar, S.; Ryu, S.; Shen, X.; Pantelides, S.T. Effects of bias on the irradiation and annealing responses of 4H-SiC MOS devices. *IEEE Trans. Nucl. Sci.* **2011**, *58*, 2925–2929. [\[CrossRef\]](#)
- Akturk, A.; McGarrity, J.M.; Potbhare, S.; Goldsman, N. Radiation effects in commercial 1200 V 24 A silicon carbide power MOSFETs. *IEEE Trans. Nucl. Sci.* **2012**, *59*, 3258–3264. [\[CrossRef\]](#)
- Green, R.; Lelis, A.J.; Urciuoli, D.P.; Litz, M.; Carroll, J. Radiation-Induced trapped charging effects in SiC power MOSFETs. *Mater. Sci. Forum* **2014**, *778–780*, 533–536. [\[CrossRef\]](#)
- Murata, K.; Mitomo, S.; Matsuda, T.; Yokoseki, T.; Makino, T.; Onoda, S.; Takeyama, A.; Ohshima, T.; Okubo, S.; Tanaka, Y.; et al. Impacts of gate bias and its variation on gamma-ray irradiation resistance of SiC MOSFETs. *Physica Status Solidi (a)* **2017**, *214*, 1600446. [\[CrossRef\]](#)
- Hu, D.; Zhang, J.; Jia, Y.; Wu, Y.; Peng, L.; Tang, Y. Impact of different gate biases on irradiation and annealing responses of SiC MOSFETs. *IEEE Trans. Electron Devices* **2018**, *65*, 3719–3724. [\[CrossRef\]](#)
- Takeyama, A.; Makino, T.; Okubo, S.; Tanaka, Y.; Yoshie, T.; Hijikata, Y.; Ohshima, T. Radiation Response of Negative Gate Biased SiC MOSFETs. *Materials* **2019**, *12*, 2741. [\[CrossRef\]](#)
- Alexandru, M.; Florentin, M.; Constant, A.; Schmidt, B.; Michel, P.; Godignon, P. 5 MeV proton and 15 MeV electron radiation effects study on 4H-SiC nMOSFET electrical parameters. *IEEE Trans. Nucl. Sci.* **2014**, *61*, 1732–1738. [\[CrossRef\]](#)
- Castaldini, A.; Cavallini, A.; Rigutti, L.; Nava, F.; Ferrero, S.; Giorgis, F. Deep levels by proton and electron irradiation in 4H-SiC. *J. Appl. Phys.* **2005**, *98*, 053706. [\[CrossRef\]](#)
- Stoller, R.E.; Toloczko, M.B.; Was, G.S.; Certain, A.G.; Dwaraknath, S.; Garner, F.A. On the use of SRIM for computing radiation damage exposure. *Nucl. Instrum. Methods Phys. Res. Sect. B: Beam Interact. Mater. At.* **2013**, *310*, 75–80. [\[CrossRef\]](#)

14. Danchenko, V.; Desai, U.D.; Brashears, S.S. Characteristics of thermal annealing of radiation damage in MOSFET's. *J. Appl. Phys.* **1968**, *39*, 2417–2424. [[CrossRef](#)]
15. Jia, Y.; Lv, H.; Song, Q.; Tang, X.; Xiao, L.; Wang, L.; Tang, G.; Zhang, Y.; Zhang, Y. Influence of oxidation temperature on the interfacial properties of n-type 4H-SiC MOS capacitors. *Appl. Surf. Sci.* **2017**, *397*, 175–182. [[CrossRef](#)]
16. Pantelides, S.T.; Wang, S.; Franceschetti, A.; Buczko, R.; Di Ventra, M.; Rashkeev, S.N.; Tsetseris, L.; Evans, M.H.; Batyrev, I.G.; Feldman, L.C.; et al. Si/SiO<sub>2</sub> and SiC/SiO<sub>2</sub> interfaces for MOSFETs—Challenges and advances. *Mater. Sci. Forum* **2006**, *527–529*, 935–948. [[CrossRef](#)]
17. Rozen, J.; Dhar, S.; Dixit, S.K.; Afanas'ev, V.V.; Roberts, F.O.; Dang, H.L.; Wang, S.; Pantelides, S.T.; Williams, J.R.; Feldman, L.C. Increase in oxide hole trap density associated with nitrogen incorporation at the SiO<sub>2</sub>/SiC interface. *J. Appl. Phys.* **2008**, *103*, 124513. [[CrossRef](#)]
18. Rozen, J.; Dhar, S.; Zvanut, M.E.; Williams, J.R.; Feldman, L.C. Density of interface states, electron traps, and hole traps as a function of the nitrogen density in SiO<sub>2</sub> on SiC. *J. Appl. Phys.* **2009**, *105*, 124506. [[CrossRef](#)]
19. Schomer, R.; Friedrichs, P.; Peters, D.; Stephani, D. Significantly improved performance of MOSFETs on silicon carbide using the 15R-SiC polytype. *IEEE Electron Device Lett.* **1999**, *20*, 241–244. [[CrossRef](#)]
20. Saks, N.S.; Agarwal, A.K. Hall mobility and free electron density at the SiC/SiO<sub>2</sub> interface in 4H-SiC. *Appl. Phys. Lett.* **2000**, *77*, 3281–3283. [[CrossRef](#)]
21. Haasmann, D.; Dimitrijević, S. Energy position of the active near-interface traps in metal–oxide–semiconductor field-effect transistors on 4H-SiC. *Appl. Phys. Lett.* **2013**, *103*, 113506. [[CrossRef](#)]
22. Jia, Y.; Lv, H.; Niu, Y.; Li, L.; Song, Q.; Tang, X.; Li, C.; Zhao, Y.; Xiao, L.; Wang, L.; et al. Effect of NO annealing on charge traps in oxide insulator and transition layer for 4H-SiC metal–oxide–semiconductor devices. *Chin. Phys. B* **2016**, *25*, 097101. [[CrossRef](#)]



© 2020 by the authors. Licensee MDPI, Basel, Switzerland. This article is an open access article distributed under the terms and conditions of the Creative Commons Attribution (CC BY) license (<http://creativecommons.org/licenses/by/4.0/>).